



Montréal, Québec
May 29 to June 1, 2013 / 29 mai au 1 juin 2013

Seismic fragility assessment of multi span continuous concrete highway bridges in British Columbia

A H M Muntasir Billah and M Shahria Alam
School of Engineering, The University of British Columbia, Kelowna, BC, Canada

Abstract: Recent seismic events all over the world have shown that bridge structures are highly sensitive and vulnerable during earthquakes. Many existing bridges were designed without adequate consideration of seismic risk. The full or partial collapse of even one major bridge in a city or community would have devastating consequences. There has been limited research to date to evaluate the seismic vulnerability of the existing bridges in British Columbia (BC) or support decision making on seismic upgrade. There is, therefore, a need for reliable methods for assessing the seismic vulnerability of existing bridges, in particular large and irregular motorway bridges having lifeline character. This research focuses on developing performance based seismic fragility curves for typical multi span continuous concrete girder (MSCC) bridges in BC. Ground motions compatible with the seismic hazard were used as input excitations for bridge vulnerability assessment. The fragility curves thus developed will quantify the vulnerability of existing MSCC bridges and aid in proper decision making to increase the safety for humans and the serviceability of vital facilities.

1. Introduction

Safety and serviceability of highway bridges, during and after an earthquake, is one of the prerequisites to ensure the continuous transport facilities, emergency, and evacuation routes during an event of extreme natural calamities. Fragility assessment provides an efficient and reliable estimate of the associated risks of highway bridges during a seismic events to a high degree of confidence. British Columbia, being the Canada's Pacific gateway, has huge impact in the overall economy of the country. The British Columbia Ministry of Transportation and Infrastructure is responsible for 900 highway structures in the highest seismic zone of Canada. There are more than 3000 highway bridges in British Columbia (BC). An earthquake of moderate intensity can result in extensive damage and a potential collapse could result from a major earthquake. Owing to the major dependence of the provinces' freight economy on highway infrastructure systems, it is critical to identify the seismically deficient bridges. A proper understanding of the seismic fragility and associated risk can provide a trustworthy estimate of the resilience of existing highway bridges. Many of the highway bridges in BC are in service for more than 30 years. Many of them were designed with codes and guidelines without the information now available on seismic safety. There is therefore, a need for reliable methods for assessing the seismic vulnerability of existing bridges, particularly large and irregular highway bridges having lifeline character.

Application of probabilistic functions also known as fragility functions have been in use over the last two decades to evaluate potential seismic risk for highway bridges, buildings, and other systems. There are more than 3000 highway bridges in BC and they vary in their types, construction material, span length, year of construction, and so forth. Based on these factors, bridges can be classified in different ways. In this particular study, analytical fragility curves were developed only for the multi-span continuous concrete girder bridge (MSCC), which represents a

significant portion of the multi-span concrete bridges in BC. The fragility curves were developed using nonlinear time history analyses of MSCC bridge models considering soil structure interaction, bearing, and abutment in the modeling. In this study, MSCC bridges located in Soil class-C (NBCC 2005), which is equivalent to soil profile Type-II in Canadian Highway Bridge Design Code (CANICSA-S6-10 2010) were considered. For this specific soil type, a set of 180 synthetic ground motion records were generated by Atkinson (2009) for magnitude-distance scenarios representative of the seismic hazard of the western Canadian region. These ground motions were used for generating the fragility curves which considered the uncertainties associated with seismic hazard. Using the results obtained from non-linear time history analyses, probabilistic seismic demand models of the bridge component, i.e. column, bearing, abutment, foundation, were developed. The component fragility curves were integrated together to develop analytical fragility curve for the MSCC bridge system.

2. Fragility curve methodology

Fragility curves allow the evaluation of seismic risk of a structure. Fragility functions describe the conditional probability, i.e. the likelihood of a structure being damaged beyond a specific damage level for a given ground motion intensity. The fragility or conditional probability can be expressed as

$$[1] \text{ Fragility} = P[LS|IM=y]$$

where, LS is the limit state or damage state of the structure or structural component, IM is the ground motion intensity measure, and y is the realized condition of the ground motion intensity measure.

In order to develop fragility curves, different methods and approaches have been developed. Depending on the available data from post-earthquake surveys and observed damage, fragility functions can be generated empirically (Yamazaki et al. 2000). However, limited damage data and subjectivity in defining the damage states limit the application of the empirical fragility curves (Padget and DesRoches 2008). In the absence of adequate damage data, fragility functions can be developed using a variety of analytical methods such as elastic spectral analysis (Hwang et al. 2000), probabilistic seismic demand model using a Bayesian approach (Gardoni et al. 2003), nonlinear static analysis (Mander and Basoz 1999), or linear/nonlinear time-history analysis (Tavares et al. 2012; Bhuiyan and Alam 2012, Ramanathan et al. 2012; Choi et al. 2004). In this study, a probabilistic seismic demand model ($PSDM$) was developed using nonlinear time-history analyses of the bridge. Using the $PSDM$, fragility curves were developed. Although this is the most rigorous method, it is also the most reliable analytical method (Shinozuka et al. 2000).

Two approaches are used to develop the $PSDM$: the scaling approach (Alam et al. 2012; Zhang and Huo 2009) and the cloud approach (Nielson and DesRoches 2007; Billah et al. 2012). In the current study, the cloud method was utilized in evaluating the seismic fragility functions of the MSCC bridge. In the cloud approach, a regression analysis is carried out to obtain the mean and standard deviation for each limit state by assuming the power law function (Cornell et al. 2002), which gives a logarithmic correlation between median EDP and the selected IM as shown below.

$$[2] \text{ } EDP = a (IM)^b \text{ or, } \ln(EDP) = \ln(a) + b \ln(IM)$$

where, a and b are unknown coefficients which can be estimated from a regression analysis of the response data collected from the nonlinear time history analyses. Effectiveness of a demand model is determined by the ability to evaluate Equation 2 in a closed form. The dispersion of the demand, $\beta_{EDP|IM}$, conditioned upon the IM can be estimated from Equation 3 (Baker and Cornell 2006).

$$[3] \beta_{EDP/IM} = \sqrt{\frac{\sum_{i=1}^N (\ln(EDP) - \ln(aIM^b))^2}{N-2}}, \quad N = \text{number of total simulation cases}$$

With the probabilistic seismic demand models and the limit states corresponding to various damage states, it is now possible to generate the fragilities (the conditional probability of reaching a certain damage state for a given IM) using Equation 4 (Nielson 2005).

$$[4] P[LS / IM] = \Phi \left[\frac{\ln(IM) - \ln(IM_n)}{\beta_{comp}} \right];$$

$\Phi[.]$ is the standard normal cumulative distribution function and

$$[5] \ln(IM_n) = \frac{\ln(S_c) - \ln(a)}{b}$$

$\ln(IM_n)$ is defined as the median value of the intensity measure for the chosen damage state, a and b are the regression coefficients of the $PSDMs$, and the dispersion component is presented in Equation 6 (Nielson 2005).

$$[6] \beta_{comp} = \frac{\sqrt{\beta_{EDP/IM} + \beta_c^2}}{b}$$

where, S_c is the median and β_c is the dispersion value for the damage states of the different components of the bridges.

Once the fragilities of the different bridge components are derived it is necessary to develop the fragility for the bridge as a system. The probability of the bridge entering or exceeding a particular limit state (LS) ($Fail_{system}$) is therefore the union of the probabilities of each of the n bridge components exceeding the same LS ($Fail_{component-i}$), and can be derived using the following union equation:

$$[7] P[Fail_{system}] = P \left[\bigcup_{i=1}^n Fail_{component-i} \right]$$

Different researchers (Choi et al. 2004; Nielson and DesRoches 2007) have used different techniques to develop system (bridge) fragility curves from component fragility curves. In this study, the system (bridge) fragility curve was developed following the approach proposed by Nielson and DesRoches (2007) through the application of joint probabilistic seismic demand model (JPSDM). This approach indicates that if one of the bridge components exceeds a particular damage state the whole bridge will encounter that level of damage and demands on the various bridge components are correlated to some extent. The failure probability of the system can be obtained with a Monte Carlo Simulation using the JPSDM and the capacity models of different components. Random samples (10^5 typically) are obtained from both the demand and the capacity model for a given seismic intensity. Probability of the demand exceeding the capacity at each intensity level is obtained and repeated for increasing values of intensity measure until the curve is defined. The lognormal parameters, median, and dispersion of the system fragility curves are then estimated using regression analysis. This methodology described in this section was used in deriving the fragility curves for MSCC bridges considering multicomponent vulnerability.

3. Bridge description and modeling

This section provides detailed information on the characteristics of the selected bridge class, and its analytical modeling procedures. Typical topological layout and structural details of MSCC bridges were identified by reviewing the database and structural drawing obtained from British Columbia Ministry of Transportation and Infrastructure. It was found that typical MSCC bridges have three to four spans and maximum span lengths in the range of 40-30m. Most of the bridges are equipped with elastomeric bearings and the abutments are mostly seat type with shallow footing foundations. Different types of bent configurations such as, wall, circular columns, and rectangular columns are available with both shallow and pile foundations. Figure 1 shows the typical MSCC girder bridge considered in this study.

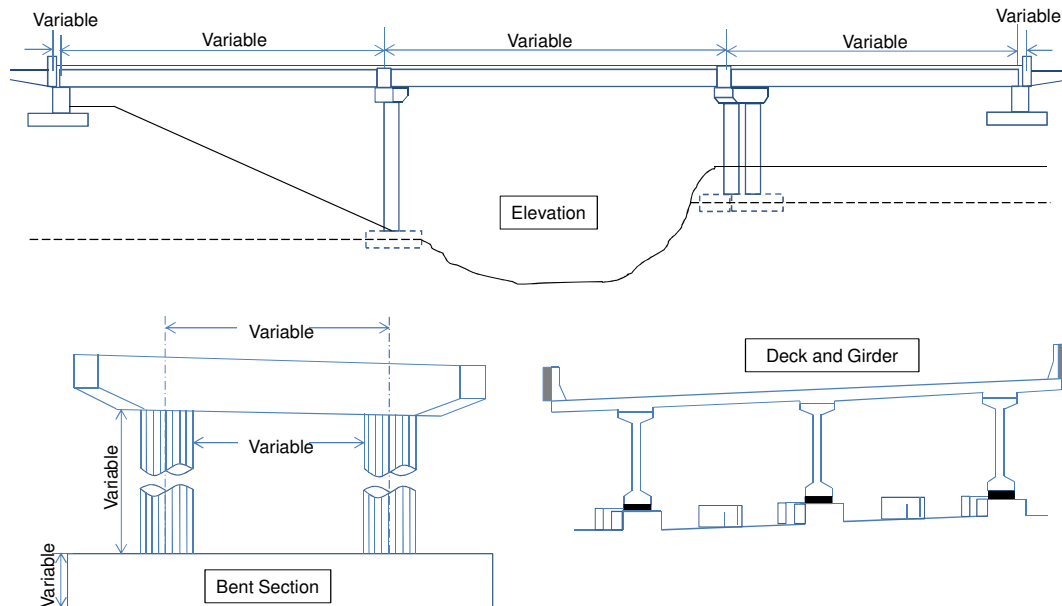


Figure 1: Configuration of a typical MSCC girder bridge in British Columbia

Using a nonlinear analysis platform, Seismostruct (Seismosoft, 2011), detailed nonlinear 3-D model of the bridge was developed. 3-D inelastic beam elements have been used for modeling the bent beams and the columns. The fiber modeling approach has been employed to represent the distribution of the material nonlinearity along the length and cross-sectional area of the member. The superstructure was modeled using elastic beam-column elements with mass lumped along the centerline. It was assumed that the deck and girder will remain elastic under seismic excitations. Highly rigid beam-column elements, referred to as rigid elements, were used to connect elements in the model. Menegotto-Pinto steel model (Menegotto and Pinto 1973) with the Filippou (Filippou et al. 1983) isotropic strain hardening property was used as the reinforcing steel material. The behavior of confined and unconfined concrete was modeled using the nonlinear variable confinement model of Madas and Elnashai (1992) that follows the constitutive relationship proposed by Mander et al. (1988). The confinement effect of the concrete section was considered on the basis of reinforcement detailing. The elastomeric bearing was idealized using a zero length spring element with a bilinear symmetric behavior in longitudinal and transverse direction. The bilinear model was defined using the initial stiffness, yield force, and post-yield hardening ratio, which were calculated following AASHTO (2007) guidelines. In order to account for the pounding between decks, contact element represented by bilinear gap element (Muthukumar and DesRoches 2006) was used. Abutments restrain the movement of bridge superstructure in both longitudinal and transverse direction through the back wall and wing wall,

respectively. The seat type abutment was modeled using the analytical model proposed by Wilson (1988). This model considers three rotational and three translational springs which represent the interaction between abutment, soil and foundation. Spring and dashpot materials, represented by zero length element, were used to model the abutment and bent foundation. The properties of the rotational and translational springs were calculated based on the linear elastic half space theory (Clough and Penzien 1975). The mass of the bent foundation was lumped at the center of the footing height.

4. Selection of ground motion

The seismic response of the MSCC bridge was evaluated using a suite of 180 synthetic ground motion generated by Atkinson (2009) for western Canada for site soil class C. The suites were generated for two different moment magnitudes M_w (6.5 and 7.5) and four different hypocentral distances (12, 25, 30 and 100 km). The uncertain characteristics of the earthquake ground motions regarding moment magnitude, intensity, and frequency contents have a great effect on nonlinear time history responses of bridge members. These ground motions were selected to represent the uncertainty associated with the ground motions. Figure 2a shows the response spectrum for the selected ground motions. Figure 2b shows the histogram of the ground motions which indicates that the selected ground motions have a wide range of PGA values which will induce inelastic response in the bridge. This set of 180 orthogonal ground motions were applied in the bridge's longitudinal and transverse direction.

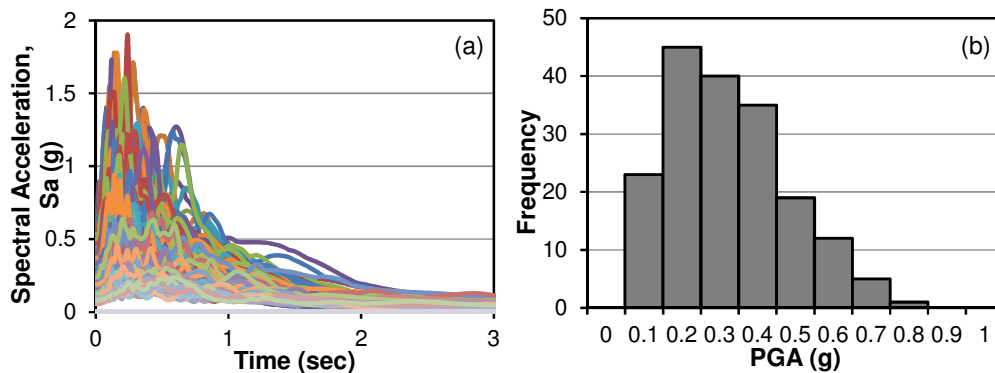


Figure 2: (a) Acceleration response spectrum and (b) Histogram of PGA values in the Atkinson (2009) ground motion suite for site soil class-C.

5. Characterization of damage states

Defining a quantitative or qualitative measure for identifying the seismic damage level is an important step in fragility assessment. Damage states (DS s) are often related to the structural capacity of a member or system and discrete in nature as they are labeled with various limiting values of considered damage index (Zhang and Huo, 2009). Damage states for bridges or components should be defined in such a way that each damage state indicates a particular level of functionality. Different forms of demand parameters are used to measure the DS of the bridge components. Previous studies (Tavares et al. 2012; Alam et al. 2012; Padgett and DesRoches 2008; Nielson and DesRoches, 2007) have shown that it is necessary to consider the vulnerability of several key components of a bridge to evaluate the vulnerability of the whole bridge. The component demand parameters considered in this study are the column displacement ductility (μ), transverse (δ_{et}) and longitudinal (δ_{el}) deformation of elastomeric bearing, deformation of abutment wing wall (δ_{ww}) and back wall (δ_{bw}).

6. Probabilistic seismic demand model

In this study, probabilistic seismic demand models (*PSDMs*) were used to establish a relationship between component demands and a ground motion intensity measure (*IM*). *PSDM* establishes a correlation between the engineering demand parameters (*EDP*) and the *IM*. Several alternative *IMs* such as spectral acceleration at the first-mode period, $S_a(T_1)$, peak ground acceleration (*PGA*), Peak Ground Velocity (*PGV*), Arias Intensity (*AI*) etc. have been developed and used for fragility assessment. Mackie and Stojadinovic (2007) and Padgett and DesRoches (2008) suggested that the peak ground acceleration (*PGA*) is the optimum choice to describe the severity of the earthquake ground motion because of its efficiency, practicality, sufficiency and hazard computability. In this study *PGA* was used as the *IM* for developing *PSDMs* and subsequently the fragility curves.

After performing the nonlinear time history analyses, peak component demands of the MSCC bridge were recorded. The *PSDMs* for different bridge components were developed by plotting the peak component responses against the *IM* for each ground motion. Finally a regression analysis was carried out to estimate a , b and $\beta_{EDP/IM}$ following equation 2 and 3. Figure 3 shows the *PSDMs* for different bridge component considered in this study. In order to develop the *JPSDM* described in section 2, correlation coefficient between the component demands were determined which are presented in Table1. These correlation coefficients describe the influence of one component over the other and reflect the dynamics of the whole bridge system. Observation of Table1 revealed that good correlation exist between the different component demand considered in this study.

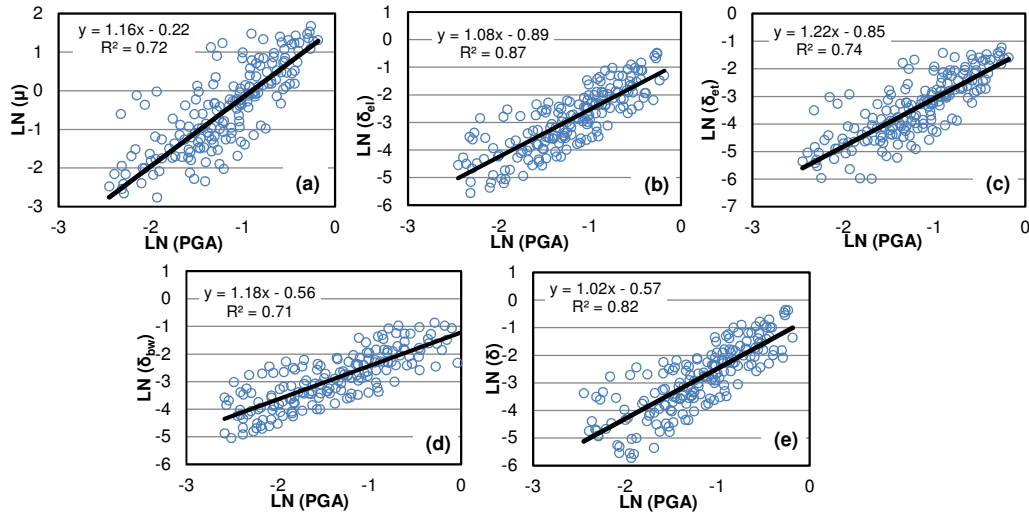


Figure 3: PSDMs for different component of MSCC bridge

Table 1: Correlation coefficients between component demands

	μ	δ_{ww}	δ_{bw}	δ_{bl}	δ_{bt}
μ	1.00	0.75	0.82	0.76	0.57
δ_{ww}	0.75	1.00	0.72	0.73	0.74
δ_{bw}	0.82	0.72	1.00	0.62	0.62
δ_{bl}	0.76	0.73	0.62	1.00	0.94
δ_{bt}	0.57	0.74	0.62	0.94	1.00

7. Limit states-capacity models

A capacity model is needed to measure the damage level of a bridge component based on prescriptive and descriptive damage states in terms of *EDPs* (Choi et al. 2004; Nielson 2005; FEMA 2003). Four damage states, as defined by HAZUS (FEMA 2003), are commonly adopted in the seismic vulnerability assessment of engineering structures, namely slight, moderate, extensive, and collapse damages. Table 2 presents the limit state capacities for the different components in terms of median (S_c) and lognormal standard deviation (β_c) which are required to describe the capacity model. The limit states of the bridge components were assumed to follow a lognormal distribution which were derived using a perspective approach (Nielson 2005). There is also uncertainty associated with each median (S_c) which must be defined. This uncertainty is given in the form of a lognormal standard deviation or dispersion (β_c). The values of lognormal standard deviation or dispersion (β_c) have been obtained following the procedure described in Nielson (2005). The values presented in Table 2 stem from the recommendations from the previous studies (Hwang et al. 2001; Nielson 2005; Padgett et al. 2008; Tavares et al. 2012; Ramanathan et al. 2012).

Table 2: Limit state capacities for different components

Component	Slight		Moderate		Extensive		Collapse	
	S_c	β_c	S_c	β_c	S_c	β_c	S_c	β_c
Column ductility	1	0.25	1.24	0.25	1.76	0.46	4.76	0.46
Elastomeric bearing-long (mm)	30	0.25	60	0.25	150	0.46	300	0.46
Elastomeric bearing- trans (mm)	30	0.25	60	0.25	150	0.46	300	0.46
Abutment wing wall (mm)	7	0.25	15	0.25	30	0.46	60	0.46
Abutment back wall (mm)	7	0.25	15	0.25	30	0.46	60	0.46

8. Component fragility curve

In order to assess the seismic vulnerability of MSCC bridge, seismic fragility curves for the piers, abutments, and elastomeric bearings were generated using the numerical results obtained from the nonlinear time history analyses. Assuming a lognormal distribution with respect to the median of seismic intensity (*PGA*), the fragility curves for different bridge component responses were generated using Equation 4 and calibrating with the capacity limit states as shown in Table 2. Figure 4 plots the fragility curves for the bridge components for the slight, moderate, extensive and collapse damage states. Evaluation of the component fragility curves offer a valuable insight on the relative vulnerability of different components on the probability of the damage.

The elastomeric bearings appear to be the most fragile components in the slight and moderate damage state while the columns and abutments are the most fragile for extensive and collapse damage state. The shift in the relative fragility of different components at different damage states can be attributed to the difference between the median values of the component limit states. For example, the median value for the elastomeric bearing in longitudinal direction is exactly 100% higher than its value for slight damage. On the other hand, this same increment is reduced to approximately 25% when considering the columns. From Figure 4 it can be noticed that, at slight damage state, the columns are the least vulnerable component while at the extensive damage they become the most vulnerable component. The shift in component vulnerability at different damage states highlights the importance of multicomponent vulnerability assessment of bridges.

9. Bridge system fragility curves

As the collapse of bridge columns and/or excessive deformation of bearings or abutments will lead to the collapse of the bridge structural system, their fragility curves should be combined to obtain the system fragility curve. The fragility curve for the bridge system was developed using JPSDM described in section 2 and using equation 7. Using a crude Monte Carlo simulation, the overall possible failure domain of the bridge was determined using the JPSDM and the limit state capacities for different bridge components. Figure 4 also shows the fragility curves of MSCC bridge class in site soil class C along with different components. Comparison of the system and component fragility in Figure 4 revealed that the bridge as a system is more fragile than any one of the bridge components. The fragility curves revealed that columns are not the most vulnerable component in a bridge which are often used to evaluate the seismic vulnerability of bridges.

The system fragility curve shown in Figure 4 were developed based on the median values of the limit state capacities. In order to consider the uncertainty associated with these median limit states, confidence bounds were established around the median fragility curves. The 90% confidence bounds were developed following the approach described in Singhal and Kiremidjian (1998). The median fragility curves along with the 90% confidence bounds are shown in Figure 5.

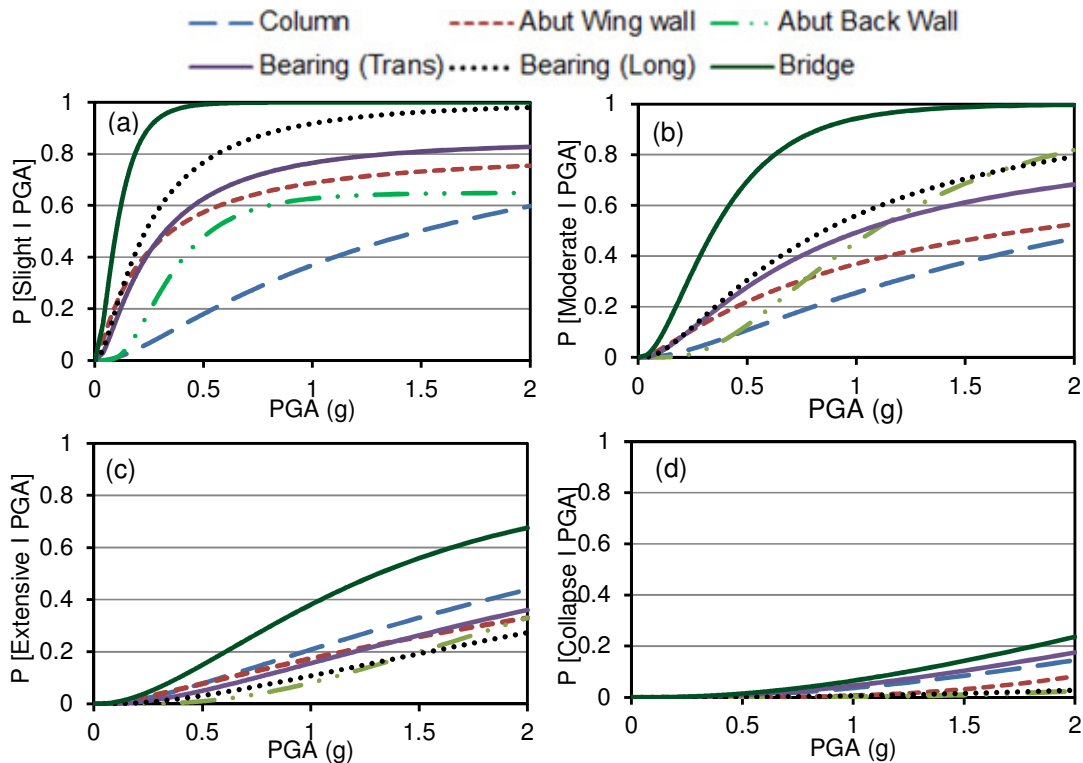


Figure 4: Bridge and component fragility curves for MSCC bridge class for (a) slight, (b) moderate, (c) extensive, and (d) collapse damage states.

From the 90% confidence bounds it can be observed that in slight and moderate damage state, the fragility curves of all confidence level were almost identical but the fragility curves of extensive and collapse damage states were much different at different confidence levels. For example, at PGA of 1g the probability of the bridge exceeding the moderate damage state varies between 94% to 97%, whereas the probability of the bridge exceeding the extensive damage state varies from 43% to 60%. The difference in the fragilities at higher damage states can be attributed to the highly nonlinear component demand at higher intensity of ground motions.

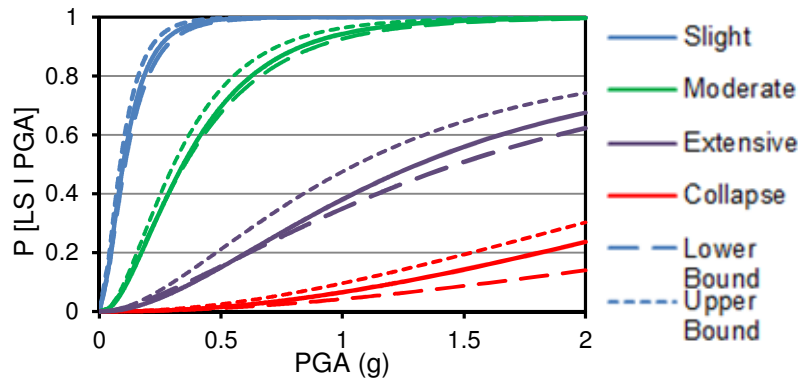


Figure 5: 90% confidence bounds and median system fragility curves for MSCC bridge class

10. Conclusions

This study utilizes analytical simulation method to conduct seismic fragility assessment of typical MSCC bridge in British Columbia. Within the scope of this study, a performance-based seismic assessment of 3D MSCC bridges, considering quantitative limit states has been carried out using probabilistic framework. Through the process, the impact of different components on the probabilistic seismic demand models, vulnerability of the MSCC bridges were evaluated. Based on the analyses result it was found that component vulnerability shifted at different damage states. Confidence bounds on the median fragility curves were established to capture the uncertainty associated with median fragility. Based on the evaluations of the representative bridge of the inventory, other bridges can be expected to behave similarly in terms of probable structural damage when they have similar structural configuration. The resulting fragility curves will provide decision makers critical information for better decision making.

Acknowledgement

The authors express their gratitude to the British Columbia Ministry of Transportation and Infrastructure and Natural Sciences and Engineering Research Council of Canada (NSERC).

References

- AASHTO. LRFD bridge design specifications, SI Units. 4th ed. Washington (DC): American Association of State Highway and Transportation Officials; 2007.
- Alam, M.S., Bhuiyan, A.R. and Billah, A.H.M.M., 2012. Seismic fragility assessment of SMA- bar restrained multi-span continuous highway bridge isolated with laminated rubber bearing in medium to strong seismic risk zones. *Bulletin of Earthquake Engineering*, 10(6): 1885-1909.
- Atkinson, G.M. 2009. Earthquake time histories compatible with the 2005 NBCC uniform hazard spectrum. *Can J Civil Eng.*;36(6):991–1000.
- Baker, J.W., Cornell, C.A., 2006. Vector-valued ground motion intensity measures for probabilistic seismic demand analysis. *PEER report 2006/08*, University of California Berkeley.
- Billah, A.H.M.M., Alam, M.S. and Bhuiyan, A.R., 2012. Fragility analysis of retrofitted multi-column bridge bent subjected to near fault and far field ground motion. In press, *ASCE Journal of Bridge Engineering*, DOI: 10.1061/(ASCE)BE.1943-5592.0000452.
- Bhuiyan, A.R., and Alam, M.S., 2012. Seismic vulnerability assessment of a multi-span continuous highway bridge fitted with shape memory alloy bar and laminated rubber bearing. *Earthquake Spectra*, 28(4): 1379-1404.

- CAN/CSA-S6-06, 2006. *Canadian highway bridge design code*, National Research Council of Canada, Ottawa; ON.
- Choi, E., DesRoches, R., and Nielson, B.G., 2004. Seismic fragility of typical bridges in moderate seismic zones. *Engineering Structures*, 26, 187-199.
- Clough RW, Penzien J. Dynamics of structures. McGraw-Hill; 1975.
- Cornell, A.C., Jalayer, F., Hamburger, R.O., 2002. Probabilistic basis for 2000 SAC federal emergency management agency steel moment frame guidelines. *J. Struct. Eng.*, 128, 526–532.
- Federal Emergency Management Agency (FEMA), 2003. *HAZUS-MH software*, Washington DC.
- Gardoni, P., Mosalam, K.M. and Der Kiureghian, A., 2003. Probabilistic seismic demand models and fragility estimates for RC bridges. *J. Earthquake Eng.*, 7(1), 79–106.
- Hwang .H., Jernigan, J.B., and Lin, Y.W., 2000. Evaluation of seismic damage to Memphis bridges and highway systems. *ASCE Journal of Bridge Engineering*, 5, 322-30.
- Hwang, H., Liu, J.B., and Chiu, Y.H. 2001. Seismic fragility analysis of highway bridges. *Mid-America Earthquake Center report: project MAEC RR-4*. Urbana: MACE.
- Mackie, K.R., and Stojadinović, B., 2007. Performance-based seismic bridge design for damage and loss limits States. *Earthquake Engineering and Structural Dynamics*, 36, 1953-71.
- Madas, P., and Elnashai, A.S., 1992. A new passive confinement model for transient analysis of reinforced concrete structures. *Earthquake Engineering and Structural Dynamics*, 21, 409-431.
- Mander, J.B., Priestley, M.J.N., and Park, R. 1988. Theoretical stress-strain model for confined concrete. *Journal of Structural Engineering*, 114(8), 1804-1826.
- Menegotto, M., and Pinto, P.E., 1973. Method of analysis for cyclically loaded R.C. plane frames including changes in geometry and non-elastic behaviour of elements under combined normal force and bending. *Symposium on the Resistance and Ultimate Deformability of Structures Acted on by Well Defined Repeated Loads*, International Association for Bridge and Structural Engineering, Zurich, Switzerland, 15-22.
- Muthukumar S, DesRoches R. A Hertz contact model with non-linear damping for pounding simulation. *Earthq. Eng. Struct. Dyn.* 2006;35:811–28.
- NBCC-2005. *National Building Code of Canada*. National Research Council of Canada, Ottawa.
- Nielson, B.G., 2005. Analytical Fragility Curves for Highway Bridges in Moderate Seismic Zones. *Ph.D. thesis*, Georgia Institute of Technology, Atlanta.
- Nielson, B.G., and DesRoches, R., 2007. Seismic fragility curves for typical highway bridge classes in the Central and South-eastern United States. *Earthquake Spectra*, 23, 615–633.
- Padgett, J.E., and DesRoches, R., 2008. Methodology for the development of analytical fragility curves for retrofitted bridges. *Earthq. Eng. Struct. Dyn.* 37, 157-74.
- Padgett, J.E., Nielson, B.G., and DesRoches, R., 2008. Selection of optimal intensity measures in probabilistic seismic demand models of highway bridge portfolios. *Earthq. Eng. Struct. Dyn.* 37, 711-725.
- Ramanathan, K., DesRoches, R. and Padgett, J.E., 2012. A comparison of pre- and post-seismic design considerations in moderate seismic zones through the fragility assessment of multispan bridge classes. *Engineering Structures*, 45: 559-573.
- SeismoSoft, 2011. SeismoStruct - A computer program for static and dynamic nonlinear analysis of framed structures, V 5.2.2 [online], available from URL: www.seismosoft.com.
- Shinozuka, M., Feng, M.Q., Kim, H.K., and Kim, S.H., 2000. Nonlinear static procedure for fragility curve development. *ASCE Journal of Engineering Mechanics*, 126, 1287-95.
- Singhal A, Kiremidjian AS. Bayesian updating of fragilities with application to RC frames. *J StructEng* 1998;124(8):922–9.
- Tavares, D.H., Padgett, J.E. and Paultre, P., 2012. Fragility curves of typical as-built highway bridges in eastern Canada. *Engineering Structures*, 40, 107–118.
- Wilson JC. Stiffness of non-skew monolithic bridge abutments for seismic analysis. *EarthqEngStructDynam* 1988;16:867–83.
- Yamazaki, F., Motomura, H., and Hamada, T. 2000. Damage assessment of expressway networks in Japan based on seismic monitoring. *Proc. of 12th World Conference on Earthquake Engineering*, CD-ROM, Paper No. 0551.
- Zhang, J., and Huo, Y., 2009. Evaluating effectiveness and optimum design of isolation devices for highway bridges using the fragility function method. *Engineering Structures*, 31, 1648-1660.